Prediction of Summer Maximum and Minimum Temperature over the Central and Western United States: The Roles of Soil Moisture and Sea Surface Temperature

ERIC J. ALFARO

Climate Research Division, Scripps Institution of Oceanography, University of California, San Diego, La Jolla, California, and School of Physics, University of Costa Rica, San José, Costa Rica

ALEXANDER GERSHUNOV

Climate Research Division, Scripps Institution of Oceanography, University of California, San Diego, La Jolla, California

DANIEL CAYAN

Climate Research Division, Scripps Institution of Oceanography, University of California, San Diego, and U.S. Geological Survey, La Jolla, California

(Manuscript received 15 March 2005, in final form 3 August 2005)

ABSTRACT

A statistical model based on canonical correlation analysis (CCA) was used to explore climatic associations and predictability of June–August (JJA) maximum and minimum surface air temperatures (Tmax and Tmin) as well as the frequency of Tmax daily extremes (Tmax90) in the central and western United States (west of 90°W). Explanatory variables are monthly and seasonal Pacific Ocean SST (PSST) and the Climate Division Palmer Drought Severity Index (PDSI) during 1950–2001. Although there is a positive correlation between Tmax and Tmin, the two variables exhibit somewhat different patterns and dynamics. Both exhibit their lowest levels of variability in summer, but that of Tmax is greater than Tmin. The predictability of Tmax is mainly associated with local effects related to previous soil moisture conditions at short range (one month to one season), with PSST providing a secondary influence. Predictability of Tmin is more strongly influenced by large-scale (PSST) patterns, with PDSI acting as a short-range predictive influence. For both predictand variables (Tmax and Tmin), the PDSI influence falls off markedly at time leads beyond a few months, but a PSST influence remains for at least two seasons. The maximum predictive skill for JJA Tmin, Tmax, and Tmax90 is from May PSST and PDSI. Importantly, skills evaluated for various seasons and time leads undergo a seasonal cycle that has maximum levels in summer. At the seasonal time frame, summer Tmax prediction skills are greatest in the Midwest, northern and central California, Arizona, and Utah. Similar results were found for Tmax90. In contrast, Tmin skill is spread over most of the western region, except for clusters of low skill in the northern Midwest and southern Montana, Idaho, and northern Arizona.

1. Introduction

There is considerable incentive to understand and predict the variability of regional surface air temperature. In the western United States, summer temperatures, especially daily extremes, dictate electrical energy usage, affect water demand, and impact agriculture and ecosystems.

Past studies on statistical seasonal prediction of surface air temperature in midlatitudes mostly used precursor sea surface temperature (SST) patterns as predictors because they tend to persist for several months (e.g., Barnett 1981; Barnston and Smith 1996). But, in summer midlatitudes the impact of SST fields on tropospheric variables appears to be modest (Koster and Suarez 2003). Barnett and Preisendorfer (1987) showed that over the contiguous United States this prediction scheme presented low skills during the summertime, suggesting that an important part of the air temperature variability remains unexplained. They also noted that the persistence of local conditions, particularly in the

Corresponding author address: Eric J. Alfaro, Escuela de Física, Universidad de Costa Rica, 2060 Ciudad Universitaria Rodrigo Facio, San José, Costa Rica.
E-mail: ejalfaro@cariari.ucr.ac.cr

western and Midwestern states, could contribute to local temperature prediction during summer.

Huang and Van den Dool (1993) and Huang et al. (1996) found that soil moisture and precipitation have an impact on the next month's near-surface air temperature in summer. Huang et al. (1996) found an inverse correlation between soil moisture and surface air temperature in the interior United States that enhanced the temperature persistence during warm season months and concluded that soil moisture is a better (local) predictor than precipitation, probably because soil moisture persists longer. Recent works (e.g., Durre et al. 2000; Van den Dool et al. 2003; Mo 2003) include soil moisture indicators to study the temperature predictability at several days to seasonal time scales over the contiguous United States. Numerical ocean–land–atmosphere climate models also include soil moisture in predicting continental temperature and precipitation (Koster et al. 2000; Koster and Suarez 2003; Yang et al. 2004). Douville (2003) explains that, because of the strong evaporation–precipitation feedback, interannual fluctuations of soil moisture over the interior North America contribute to the predictability of temperature in the lower troposphere during summer.

Most of the studies cited in the previous paragraph focused on average summer temperature, except for Durre et al. (2000), which investigated summertime daily maximum temperature and their extremes. However, because the atmospheric surface layer and its attendant mechanisms are quite different during day and night, we are motivated to consider if the climatic linkages and predictive skill differ for maximum temperature (Tmax) versus those for minimum temperature (Tmin). Additionally, the set of users and applications requiring forecasts of Tmax may be quite different from those for Tmin. Although fluctuations in Tmax and Tmin are significantly correlated, the variability of Tmax is larger than that of Tmin for nearly all locations during nearly all seasons (Fig. 1). This is especially true in summer, when the mean standard deviation of Tmax is approximately 30% larger than that of Tmin. As will be brought out, the predictive linkages and patterns associated with these two variables have some important differences.

The goal of this paper is to quantify and understand the predictability of continental maximum and minimum surface air temperature during summer over a broad midlatitudinal region covering the central and western half of the United States. We also consider predictability of seasonal frequency of daily Tmax extremes. Based on results from previous studies, we employ Pacific SST (PSST) and a soil moisture index, the Palmer Drought Severity Index (PDSI), to predict

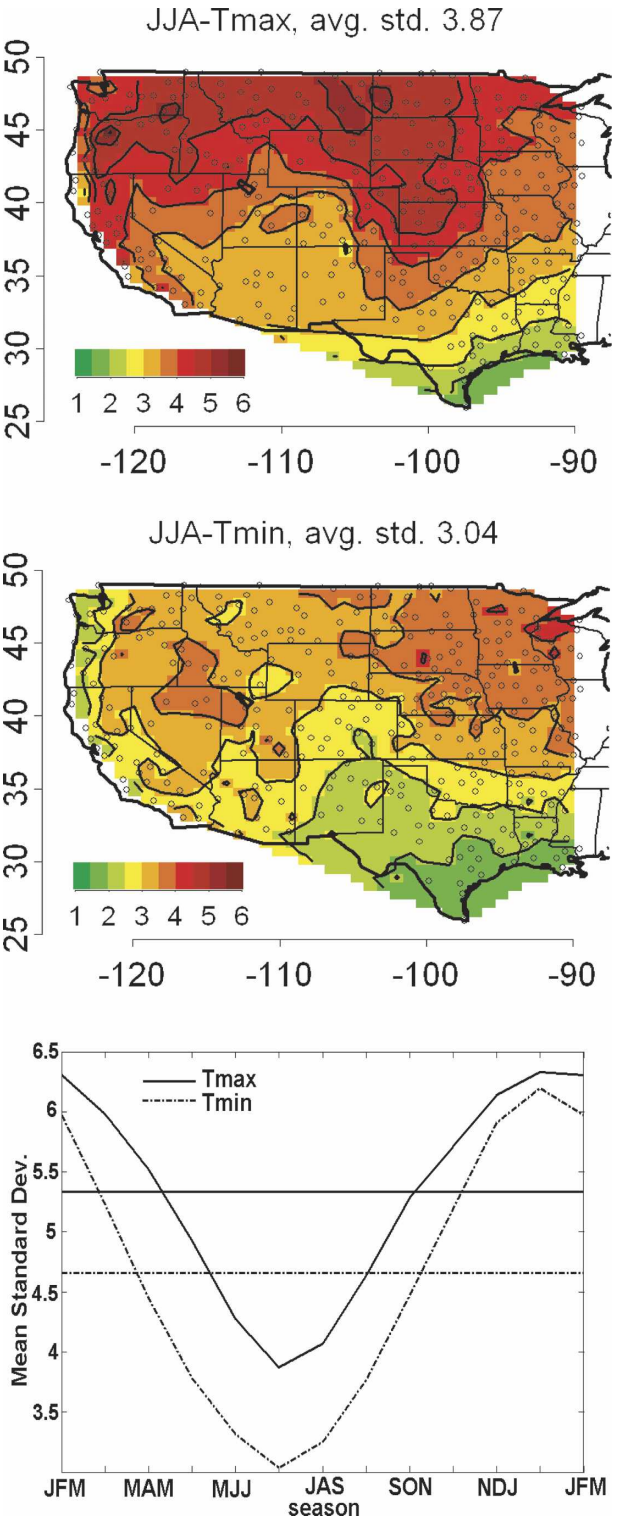

FIG. 1. Standard deviation (°C) mapped for (top) Tmax and (middle) Tmin for summer (JJA) daily data from 1950 to 2001. Contours are every 0.5°C. (bottom) Average over the entire domain of the standard deviation (°C) of Tmax (solid) and Tmin (dashed) for each season.

maximum and minimum temperatures. Our analysis focuses on the summertime, but for comparison also examines other seasons. The paper is organized as follows. After a description of the data used in the next section, section 3 describes the methodology. Variability of Tmax and Tmin is discussed in section 4. Specification of temperature from PSST and PDSI is described in section 5, including diagnostic analysis and the prognostic models as well as the seasonal cycle of field-averaged skill (FAS). Results for temperature prediction are presented in section 6, including comparison of predictive skill in summer with that obtained for other seasons. Finally, the summary and conclusions are presented in section 7.

2. Data

Each of the datasets employed covered the common time period 1950–2001. The predictands were formed from surface air temperature records from the National Climatic Data Center (NCDC) first-order and cooperative observer summary of the day dataset, known as DSI-3200 (NCDC 2003). These data were used and described recently over the contiguous United States by Groisman et al. (2004). From DSI-3200, 711 stations were preselected with 1% or less missing data in their maximum and minimum temperature records (Tmax and Tmin, respectively) over the central and western half of the contiguous United States (25.0°–50.0°N, 89.5°–124.5°W). The domain considered includes portions of the Midwest and south-central and southern states, the Great Plains, and all 11 of the western mountainous states. This domain, while focusing on the West, facilitates comparison with previous studies of air temperature predictability (e.g., Barnett and Preisendorfer 1987; Huang et al. 1996; Koster and Suarez 2003; Mo 2003). The full set of stations was decimated to produce an array of stations that were separated by a radial distance of 0.7° or more, obtaining a subsample of 350 stations (circles in Fig. 1). This decimation alleviated a sampling bias toward higher density of stations in the eastern part of the domain. Three predictand variables were considered, including seasonally averaged Tmin and Tmax, and the seasonal frequency of daily Tmax extremes (Tmax90) defined as the frequency of daily Tmax warmer than the 90th percentile of the local summertime climatology of daily Tmax.

Two datasets were used as predictor fields. First, Pacific basin (7.5°S–62.5°N, 112.5°E–82.5°W) SST anomalies on a 5° × 5° grid are from the optimally interpolated statistically homogenous concatenation of Kaplan et al. (1998) and Reynolds and Smith (1994) analyses obtained from the International Research Institute for Climate Prediction (IRI). Second, 194 National Climatic Data Center Climate Division PDSI (Palmer 1965; Alley 1984; Heddinghaus and Sabol 1991; Heim 2002; Lawrimore et al. 2002) time series cover the central and western United States (circles in Figs. 3d,e,f represent the centroid of these climate divisions). Hereinafter these datasets are referred to as PSST and PDSI, respectively. PDSI is a commonly used and reasonably good measure of soil moisture and other hydrological conditions at the land surface (Dai et al. 2004). Durre et al. (2000) noted that the relationship between soil moisture and the subsequent monthly temperature is robust with respect to both the analysis method and the soil moisture parameter used, including PDSI. A detailed description of the PDSI formulation can be found in Heim (2002) and Shabbar and Skinner (2004).

3. Methodology

Following the statistical approach described by Gershunov and Cayan (2003), canonical correlation analysis (CCA) is used here to match patterns in the predictor fields with patterns in the predictand field. This methodology is employed in both the specification (contemporaneous) and the prediction (time lagged) experiments. In this approach, CCA relates the contemporaneous and/or antecedent observations of the predictor fields (PSST and/or PDSI) to the observed seasonal values of daily Tmax, Tmin, and Tmax90 fields. One underlying hypothesis is that Pacific SST anomaly patterns force large-scale atmospheric circulation, which influences local surface air temperature anomalies. A second hypothesis is that local temperature variability is modulated by soil moisture through the interplay between latent and sensible heating from the land surface (Mo 2003). The resolved PSST and PDSI anomalies span a range of variability, from seasonal to interannual to multidecadal time scales.

The statistical prediction approach (see Gershunov and Cayan 2003 for details) consists of three steps. First, the predictor and predictand fields are prefiltered with the same number of p principal components (PCs) each. Second, patterns of variability in the predictor and predictand fields represented by their respective p PCs are related to each other via q canonical correlates derived from CCA. Finally, the optimal statistical model is defined by considering cross-validated measures of skill for all reasonable combinations of p and q. The optimum p and q values were chosen as the combination giving the maximum average skill over the analysis domain.

The number of modes for specification and prediction models was optimized in a separate module, so the

number of modes used in the specification is not necessarily the same as the number of modes used in the prediction. It is important to note that the optimal p–q model is approximate, because the p and q values are selected from a rather smoothly varying surface of model performance. Similar-complexity models from nearby p–q pairs will give approximately the same predictive skill. In practice the number, p, of patterns and, q, of relationships selected ranged from 2 to 17. Because all skill calculations are cross validated, the results should provide realistic estimates of temperature forecast skill obtainable using linear combinations of PSST and/or PDSI predictors.

4. Variability structure

To explore relationships of Tmax and Tmin with local soil moisture variability, represented by PDSI, simultaneous June–August (JJA, hereafter 3-month periods are denoted by the first letter of each respective month) correlations were calculated between Tmax and Tmin, Tmax and PDSI, and Tmin and PDSI (Fig. 2). As expected at seasonal time scales, correlations between Tmax and Tmin yield positive values for practically all stations (Fig. 2a), although some regions exhibit much stronger correlations than others, reinforcing the notion that different local mechanisms may be at play during daytime than during nighttime.

A consistent pattern of negative correlation is obtained between Tmax at stations and their nearest Climate Division PDSI time series (Fig. 2b), indicating that dry conditions tend to be accompanied by higher maximum (day time) temperatures, and vice versa (PDSI describes drought severity with increasing magnitude in the negative direction). This association is strongest over most states in the eastern part of the domain and near the junction of Idaho, Wyoming, Utah, and north-central Montana. The central United States was identified by Huang et al. (1996) and Koster and Suarez (2003) as a region of maximum variability in summer soil moisture and evaporation, perhaps an indication of a strong land surface influence on surface air temperature. Mo (2003) found that this region is associated with the largest mean temperature variability in the United States.

The analogous map of correlations for Tmin with PDSI (Fig. 2c) also shows a pattern of negative correlations, but the absolute values are mostly smaller than those obtained for Tmax. These results show that in spite of positive summer correlation between Tmax and Tmin, anomalous PDSI explains more local variance of Tmax than of Tmin. Results from Fig. 2 are consistent with those of Durre et al. (2000), who stated that "re-

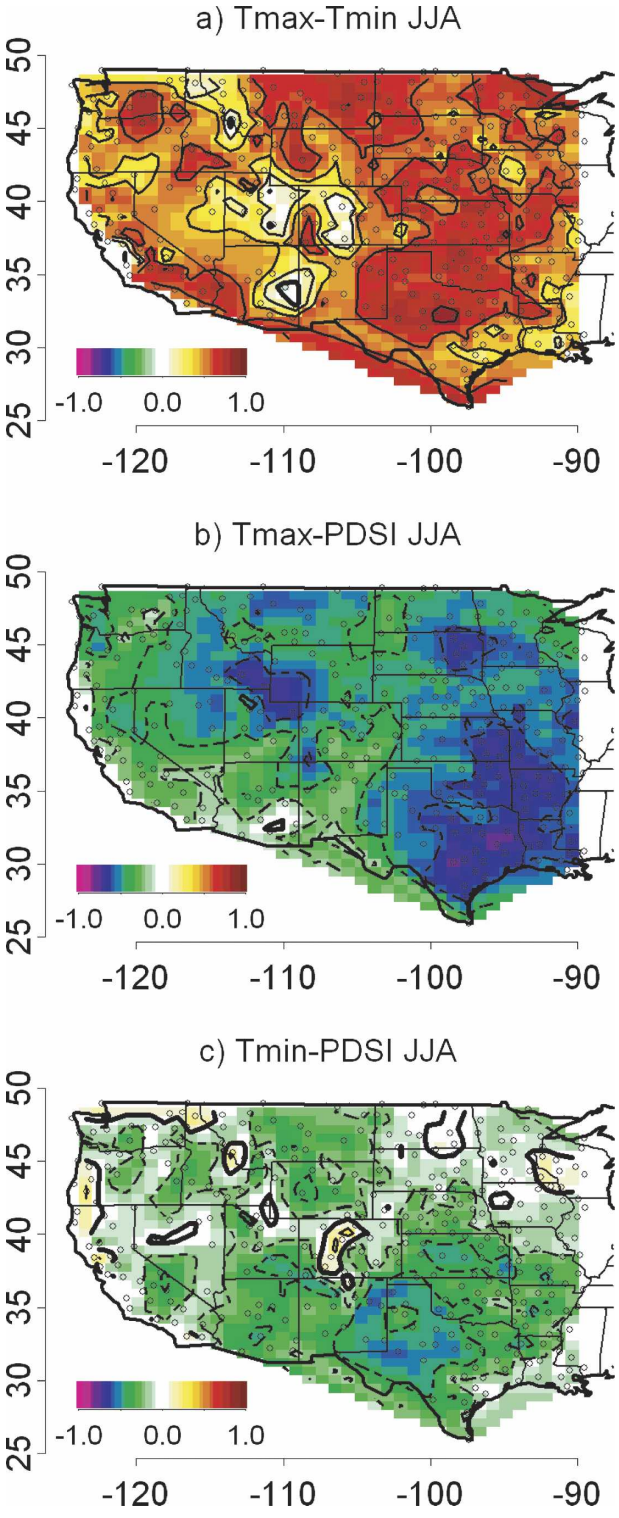

FIG. 2. Simultaneous JJA correlations between (a) Tmax and Tmin, (b) Tmax and PDSI, and (c) Tmin and PDSI. Station temperatures were correlated with PDSI at the nearest climate division. All correlation patterns are displayed in color on the common scale (−1: violet; 1: dark red). Zero contours are thickened. Correlations are also displayed as contours at 0.2 intervals. Negative contours are dashed, and positive are solid. Small circles represent station locations.

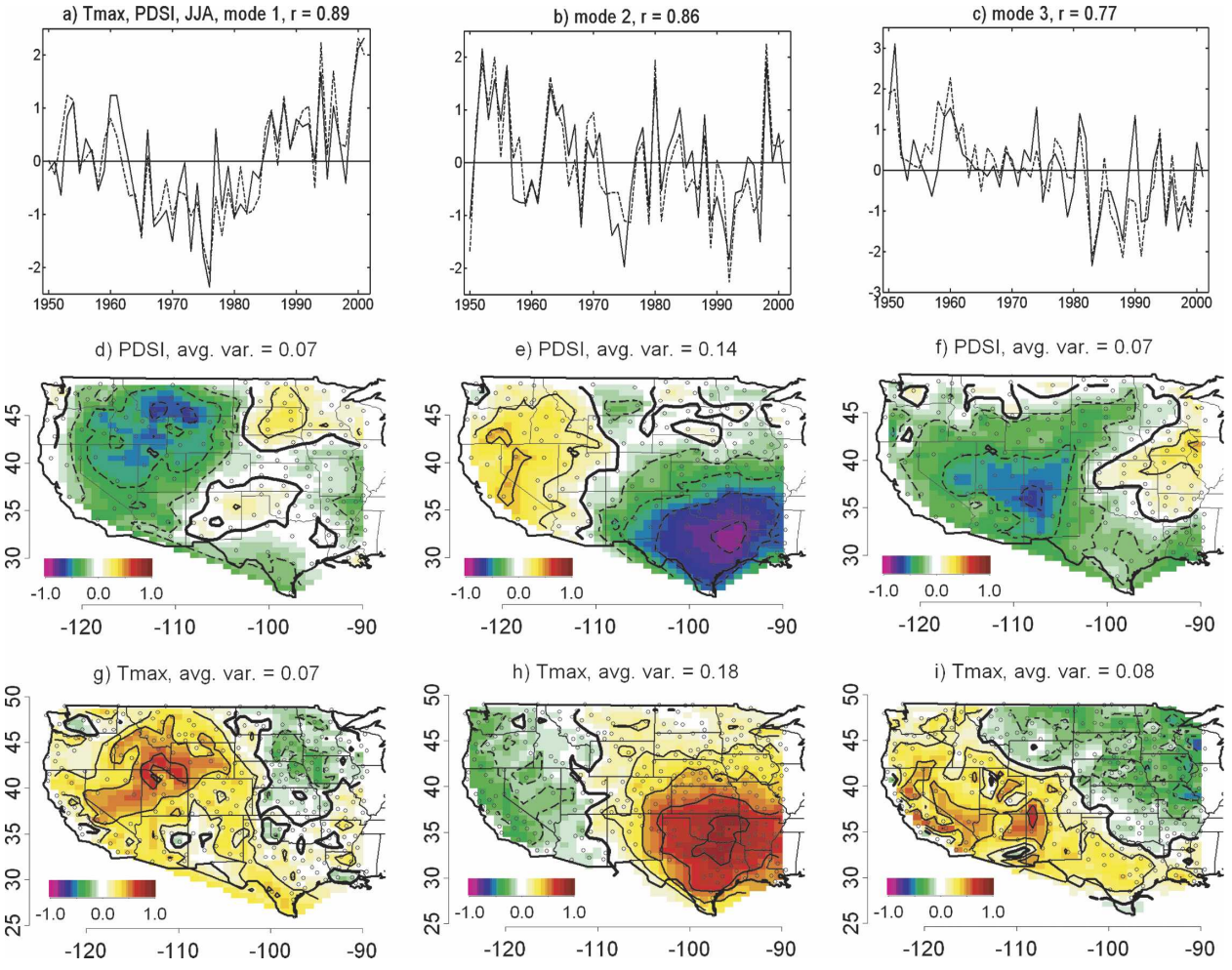

FIG. 3. First three CCA modes of JJA Tmax with PDSI. Time series of the first three CCA modes: predictor (solid) and predictand (dashed); the correlations between the series are (a) 0.89, (b) 0.86, and (c) 0.77. (d), (e), (f) Spatial patterns of PDSI predictor fields and (g), (h), (i) Tmax as predictand are displayed as correlations of the CCA mode time series with their respective variable fields at each location represented by the small circles (i.e., climate division for predictors and station for the predictand). Correlation values are represented by color scale (−1: violet; 1: dark red), and by contours (0.2 intervals) with zero contours thickened. Negative contours are dashed, and positive are solid (avg. var. means the average variance).

sults for warm-season months indicate that, particularly for inland nonarid areas, a wet soil tends to depress the concurrent and subsequent monthly mean temperature, while a drier-than-normal soil is favorable for higher-than-expected monthly mean temperatures," but since evapotranspiration occurs primarily during the day, "it follows that daytime temperatures should be more sensitive to variations in soil moisture than nighttime temperatures." This daytime-versus-nighttime asymmetry is clearly verified by Fig. 2.

5. Specification analysis

a. Simultaneous summer patterns

Before examining skill, we use CCA in a diagnostic mode to examine JJA simultaneous patterns relating PSST and/or PDSI to Tmax or Tmin. Diagnostic CCA analysis suggests that summer Tmax variability is mainly driven by contemporaneous soil moisture conditions over the central and western United States, while Tmin variability is better explained when PSST and PDSI fields are used jointly. These results are illustrated in Figs. 3–4 (we show only the first three modes in Figs. 3, 4, 7, and 8 because the spatial structures associated with the less correlated higher-order modes become progressively less spatially coherent).

Figures 3a,b,c show the first three leading CCA modes of PDSI and Tmax. Negative PDSI correlations (Figs. 3d,e,f) are in local agreement with positive Tmax correlations (Figs. 3g,h,i). From the three modes plotted, the second mode shows the greatest PDSI (Tmax) average variance with a lobe of high negative (positive)

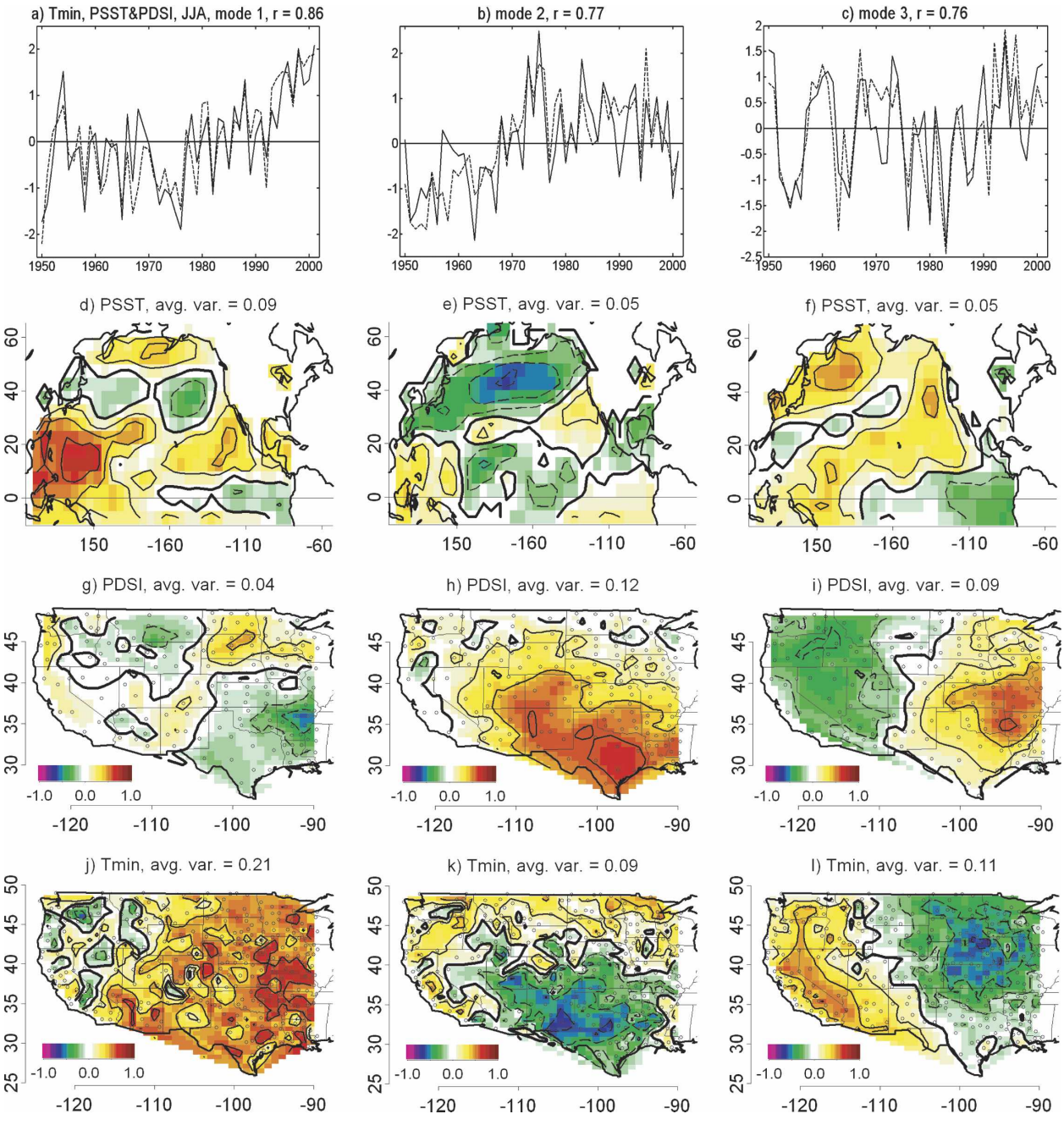

FIG. 4. First three CCA modes of JJA Tmin with PSST and PDSI. Time series of the CCA modes: predictor (solid) and predictand (dashed); the correlations between the series are (a) 0.86, (b) 0.77, and (c) 0.76. Spatial patterns of (d), (e), (f) PSST and (g), (h), (i) PDSI predictor fields and (j), (k), (l) Tmin as predictand are displayed as correlations of the CCA time series with their respective variable fields at each location (i.e., grid cell or climate division for predictors and station for the predictand, with these last two represented by the small circles). Correlation values represented by color scale (−1: violet; 1: dark red), and also as contours at 0.2 intervals, with zero contours thickened. Negative contours are dashed, and positive are solid (avg. var. means the average variance).

correlations over the southeastern states of our domain. The spatial concordance and negative correlation between PDSI and Tmax patterns is consistent with the local correlations in Fig. 2b and indicates that mechanisms conducive to dry or wet conditions are very strongly biased toward higher or lower maximum temperatures. Durre et al. (2000) explain this association by a feedback in which "a depletion in the amount of water in the soil that is brought about by a deficit in precipitation causes the rate of surface evapotranspiration

to decrease." The reduced evapotranspiration favors the sensible heat flux, "which requires a warmer surface and planetary boundary layer. The higher temperatures, in turn, tend to enhance the drying of the soil and lower atmosphere . . . particularly during summer, when the surface latent heat flux tends to be large."

The leading three modes of jointly considered PSST and PDSI and Tmin are presented in Fig. 4. From the three modes plotted (Figs. 4a,b,c), the average variance of the first mode associated with PSST (Fig. 4d) is higher than the one associated with PDSI fields (Fig. 4g). It shows the greatest Tmin average variance with a robust positive Tmin correlation pattern at longitudes east of 110°W (Fig. 4j). In contrast to the first mode, the correlation patterns of Tmin associated with the second and third joint PSST and PDSI modes (Figs. 4k,l) resemble the PDSI-only modes (not shown for Tmin) (Figs. 4h and 4i, respectively). The average variance of the Tmax modes that can be attributed to PDSI was also higher than the variance attributed to PSST (not shown). However, Tmin correlation patterns suggest that both PSST and PDSI fields contribute strongly to explain the Tmin variance.

b. *Simultaneous models of Tmax and Tmin variability*

The summer specification skill of the CCA models is presented in Fig. 5, which shows maps of the cross-validated correlations between observed and statistically estimated JJA Tmax and Tmin. We notice from Figs. 5a,b that PDSI and PSST and PDSI explain a significant portion of the summer Tmax and Tmin variability, respectively. For both Tmax and Tmin, the model estimates have a statistical significance greater than the 99% confidence level. Some important differences appear though, for example, Tmax has lowest skill in the interior southwestern states, while Tmin has lowest skill in the interior north-central portion of the domain. The low Tmax skill region (Fig. 5a) coincides with the area affected by the southwest monsoon that can influence summer PDSI and reduce its local coupling with Tmax (see also Fig. 2b). The region of low Tmin (Fig. 5b) over the mountainous West is decoupled from remote SST influences as well from local PDSI (see also Fig. 2c).

To compare the summer season results with other periods of the year, the Tmax and Tmin specification and prediction model calculations were repeated for each of the other seasons. Field-averaged specification skill for each season, for each of the three predictor fields, is displayed in Fig. 6. This exercise also generated predictive model skill for each season at lags of 1, 3, and 5 months, as will be described in the next section.

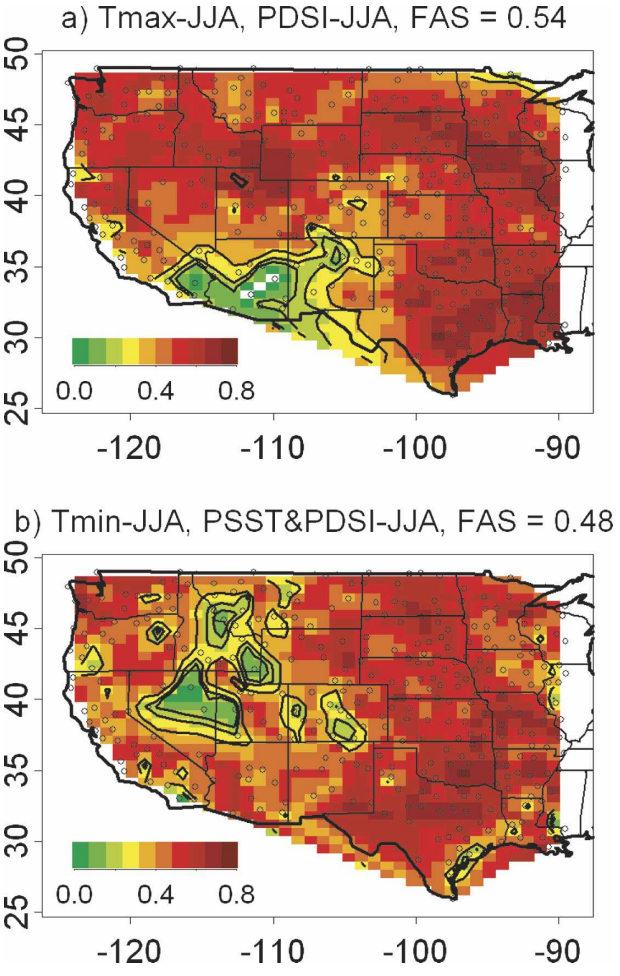

FIG. 5. JJA Tmax and Tmin specification skill expressed as correlations between the cross-validated forecast and observations. Uncolored areas are regions of insignificant negative correlations. (a) Tmax using PDSI and (b) Tmin using PSST–PDSI as predictor field, respectively. The three contours plotted surround and represent the 90th, 95th, and 99th percent levels of significance in order of increasing correlations.

As we mentioned in section 3, the *p–q* pairs for the different CCA models were chosen as the model complexity giving the maximum average skill over the analysis domain, and it is not necessarily the same as that for the summer case.

Figure 6 shows some important differences between Tmax and Tmin, regarding their PSST and PDSI linkages. For Tmax, during the period from spring to early fall (from FMA to ASO), the average skills are very similar from models that included PDSI-only or PSST and PDSI predictors. Furthermore, Tmax skills from the PSST-only models are lower. This indicates that during the warm season at zero time lag, local effects associated with the availability of soil moisture rather than remote or indirect effects from PSST are the dominant control of Tmax variability. This result is consis-

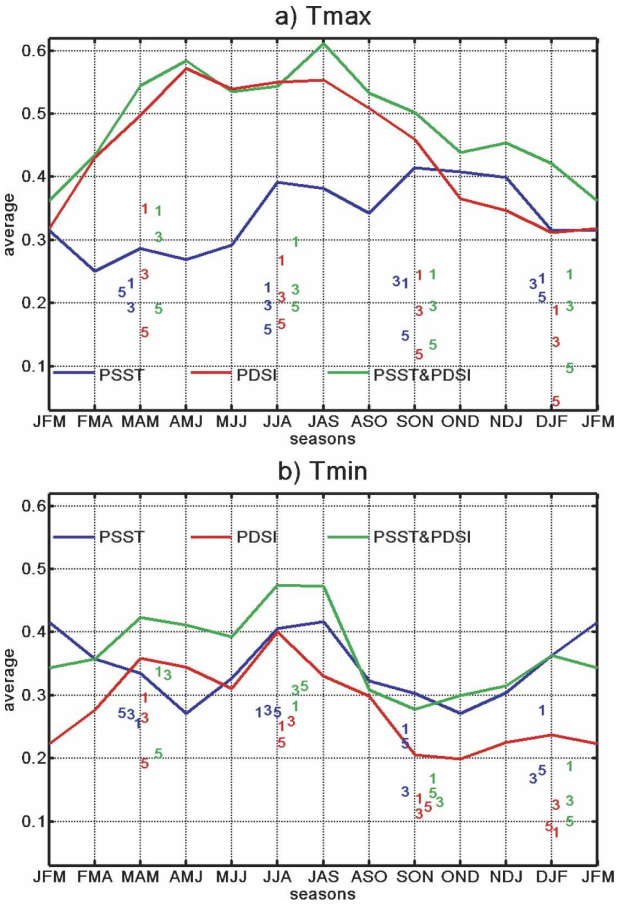

FIG. 6. Annual cycle of (a) Tmax and (b) Tmin specification skill. They are shown as the field-average skill (FAS) from the optimal complexity model (see text and Gershunov and Cayan 2003) for all 12 three-month seasons based on three different sets of predictors: PSST (blue line), PDSI (red line), and PSST and PDSI (green line). Using the same colors for the different set of predictors, the numbers represent the FAS of the prediction experiments for 1-, 3-, and 5-month lead times before the beginning of the MAM, JJA, SON, and DJF seasons.

tent with Huang et al. (1996), who found that warm season months produced the highest correlations between lagged soil moisture and station Tmax. Local control and seasonal variability of Tmax associated with soil moisture can be explained through the Delworth and Manabe (1988, 1989) studies. They showed that soil moisture contains variance on seasonal to interannual scales and that an increase (decrease) of soil moisture tends to increase (decrease) the latent heat flux and therefore atmospheric moisture, while decreasing (increasing) the sensible heat flux, and therefore air temperature. This scheme is especially valid for seasons and nonarid locations where the ratio of potential evaporation to precipitation is greater than one and there is ample energy for the removal of moisture from the surface by evaporation (see also Durre et al. 2000).

The results here indicate that in seasons from SON to JFM, both large scale and local forcings (PSST and PDSI) contribute to the variance of Tmax fields. Better skill was generally obtained using PSST and PDSI fields during fall and winter for Tmax predictions. Seasonal differences in the large-scale (i.e., SST) control on Tmax stem from the following facts: (a) tropical teleconnections are strongest in the winter hemisphere; (b) ENSO phase evolution is characterized by a distinct seasonal cycle; and (c) North Pacific transient cyclone and anticyclone activity, related to large-scale Pacific SST patterns, is more vigorous and penetrates deeper inland during winter.

The results demonstrate that Tmax can be specified with a higher degree of skill than can Tmin for all seasons of the year (Fig. 6b). During MAM–JAS the highest Tmin specification skills were obtained when PSST–PDSI fields were used as predictors, but notice that the difference between Tmin average skill values using PSST or PDSI is not as great as those obtained for Tmax during these seasons. This suggests that nighttime temperatures are controlled by local *and* large-scale factors during spring and summer in the central and western United States. For the remainder of the year, ASO–FMA, Tmin specifications are mostly controlled by PSST. Low skill obtained from PDSI-only predictors during fall and winter indicates that the influence of soil moisture on Tmin predictions becomes minimal during the cool season. During the cool season, soil moisture's influence on Tmin is less important than in the warm season, probably because humidity and, therefore, greenhouse trapping, is more associated with advection than local evaporation.

6. Predictive relationships

The same procedure as for the contemporaneous linkages was applied to examine predictive skill at one month to several months time lead. The field-averaged skills for time leads of 1, 3, and 5 months before the beginning of the MAM, JJA, SON, and DJF seasons are shown in Fig. 6. For each of the time leads, JJA Tmax and Tmin were better predicted by PSST and PDSI fields than from either individual predictor field.

a. Lagged patterns

Figures 7a,b,c show the first three leading modes of May PSST and PDSI and JJA Tmax. Notice that PSST average variance associated with the two first modes is low when compared with the third mode (Figs. 7d,e,f). The first mode shows the greatest Tmax average variance with two lobes of opposite sign pivoting around 105°W. This pattern also resembles the PDSI correla-

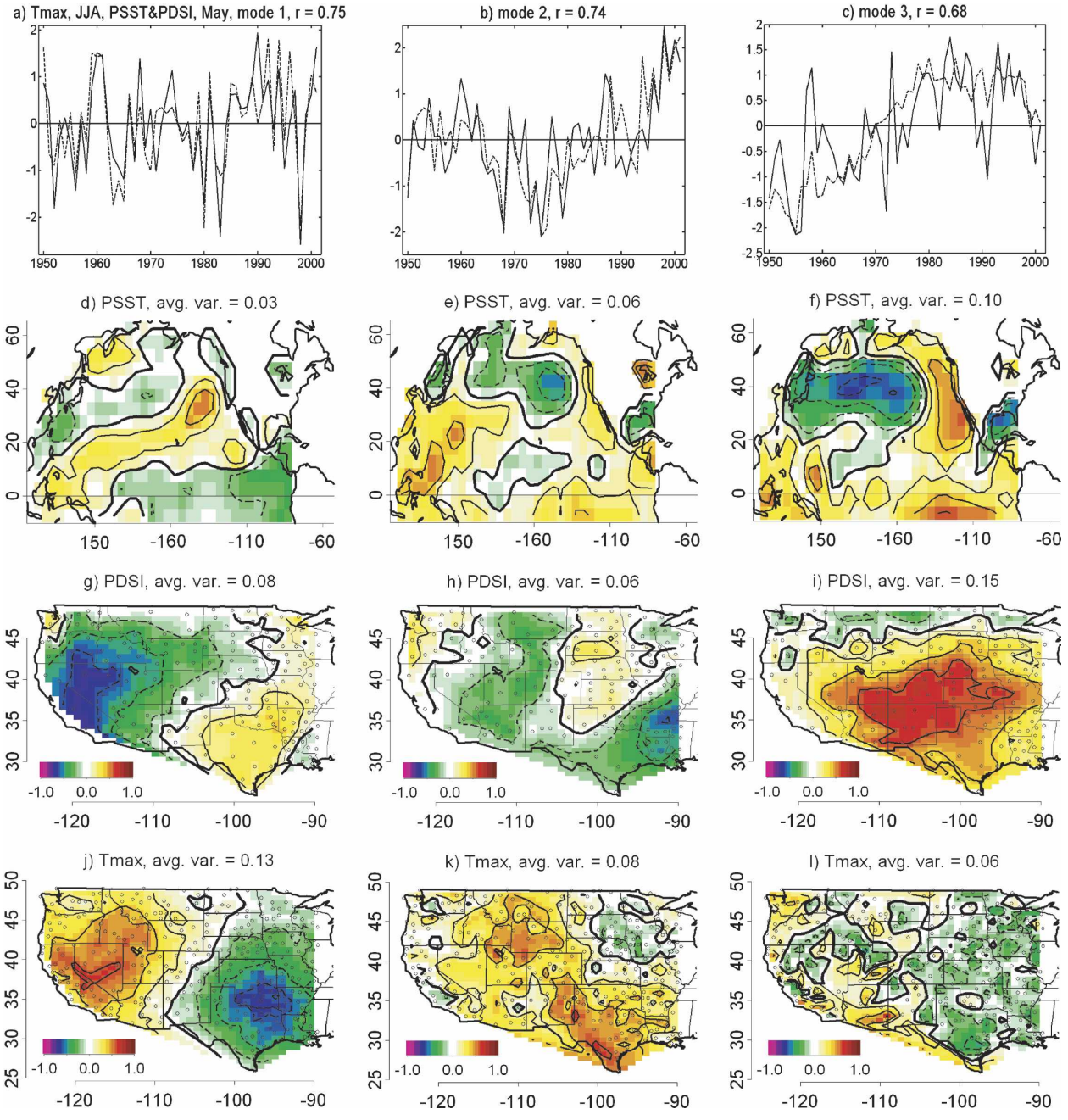

FIG. 7. Same as in Fig. 4, but for JJA Tmax with May PSST–PDSI. The correlations between the series are (a) 0.75, (b) 0.74, and (c) 0.68.

tion in Fig. 2. To determine if the leading predictor modes are associated with known large-scale features, they were correlated with May values of prominent indices of climate variability, such as the Pacific decadal oscillation (PDO) and Niño-3.4. Modes 1 and 2 of PSST–PDSI did not exhibit any substantial correlations with those indices (Table 1a), supporting the previous results that Tmax is mostly controlled by local land surface characteristics. Mode 3 had a correlation of 0.75 [statistical significance of 99%, according to Ebisuzaki (1997)] with the May PDO index. PDO is the dominant mode of anomalous SST variability in the extratropical North Pacific (Mantua et al. 1997). This result indicates that the coupled variability between JJA Tmax and May climate is in part due to low-frequency modes such as the PDO. However, little Tmax variability is ex-

TABLE 1. Correlations between the PSST–PDSI modes plotted in (a) Fig. 7 and (b) Fig. 8 and the described index values observed in May for 1950–2001.

(a)	Mode	Index: PDO	Index: Niño-3.4
	1	−0.05	0.19
	2	−0.29	−0.21
	3	0.75**	0.30*

(b)	Mode	Index: PDO	Index: Niño-3.4
	1	−0.61**	−0.24
	2	−0.49**	−0.25*
	3	−0.14	−0.56**

* Has a statistical significance greater than 95% level according to Ebisuzaki (1997).
** Has a statistical significance greater than 99% level.

plained by this mode (Fig. 7l); it seems to mainly account for the coastal versus inland Tmax gradient probably mainly through the near-coast SST expression of the PDO. Although the associated PDSI pattern is strong (Fig. 7i), it does not account for local Tmax predictability. This is probably because (a) local persistent PDSI conditions are not strongly correlated with Tmax in this southwestern desert and mountainous region (Fig. 2b) and (b) PDSI May –JJA persistence may be weak there due in part to the influence of the southwestern monsoon.

The results obtained for JJA Tmin from May PSST–PDSI predictors (Figs. 8a,b,c) are different from those obtained for JJA Tmax. The PSST correlation map of the leading mode resembles the PDO structure (Fig. 8d, cf. also with Fig. 7f) and has a correlation with May PDO index of −0.61 (Table 1b; statistically significant at the 99% level). In contrast to the Tmax results (Fig. 7l), the first Tmin mode displays weak correlations with PDSI. The greatest Tmin variance explained is represented by a lobe of positive correlation in the central southwest of the domain (Fig. 8j). The second Tmin mode has stronger correlations with PDSI; the high PDSI average variance portrayed in Fig. 8h has a similar spatial structure as Fig. 7i but is locally stronger around the Four Corners region where it couples strongly with subsequent summer Tmin variability. The third Tmin mode has a correlation with Niño-3.4 index of −0.56 (Table 1b; significant at 99%) and is associated with the greatest PSST variance of the three modes plotted (Fig. 8f). The associated PDSI spatial dipole pattern anticorrelates locally with subsequent summer Tmin (Figs. 8i,l) explaining significant variance in the extreme southwest and the southern Great Plains.

b. Prognostic models: Predictability at 1 to 5 months

To directly explore summertime temperature predictability based on the kinds of climatic couplings exemplified in section 6a, summer Tmax skill (i.e., cross-validated correlation coefficient between prediction and local observation) is mapped for CCA models using antecedent May PSST and/or PDSI predictors (Fig. 9). Much of the predictability that extends from California to the interior western north and central domain (Fig. 9a) is mainly due to PSST (Fig. 9b) and to a lesser extent to PDSI fields (Fig. 9c). Similar skill maps were obtained by Barnett and Preisendorfer (1987) for June mean temperature prediction based on persistence and also for August mean temperature predicted from antecedent PSST. The region of relatively high skill over the Midwest and Plains states in the study conducted here is mainly associated with PDSI, while PSST contributes very little predictability. This is consistent with the results of Mo (2003), who also found maximum summer mean temperature predictability over Texas and Oklahoma using antecedent soil moisture predictors. Douville (2003) illustrates that variability of local surface evaporation plays a significant role in the lower-troposphere energy budget in the interior of the United States. The Midwest, Great Plains, and Rocky Mountain states were identified by Durre et al. (2000) as regions in which the probability of warm Tmax is significantly elevated during dry spells. The interior northwestern and west south-central states retain significant JJA Tmax predictability using March PSST and PDSI predictors (map not shown). Again the first mode mainly related to PSST and the second mode mainly related to PDSI. For the rest of the area, skills are relatively weak for the March prediction models.

Prediction skill maps for JJA Tmin fluctuations are presented in Fig. 10. In contrast to Tmax, which featured maximum skill in California, most of the Pacific Coast region is well predicted (Fig. 10a) from May predictors. There is also relatively high Tmin skill in the North American monsoon region (e.g., Higgins et al. 2003) using May PSST and PDSI predictors. The Tmin skill in the monsoon region is similar to that found for mean temperature by Mo (2003) using winter and spring SST predictors. In the present case, May PSST appears to be the main contributor to skill of JJA Tmin fluctuations (Fig. 10b), but PDSI also contributes in a scattered fashion to skill within the regions described above (Fig. 10c). Testimony to the powers of persistence, March, April, and even January PSST and PDSI predictors account for similar predictability as do the

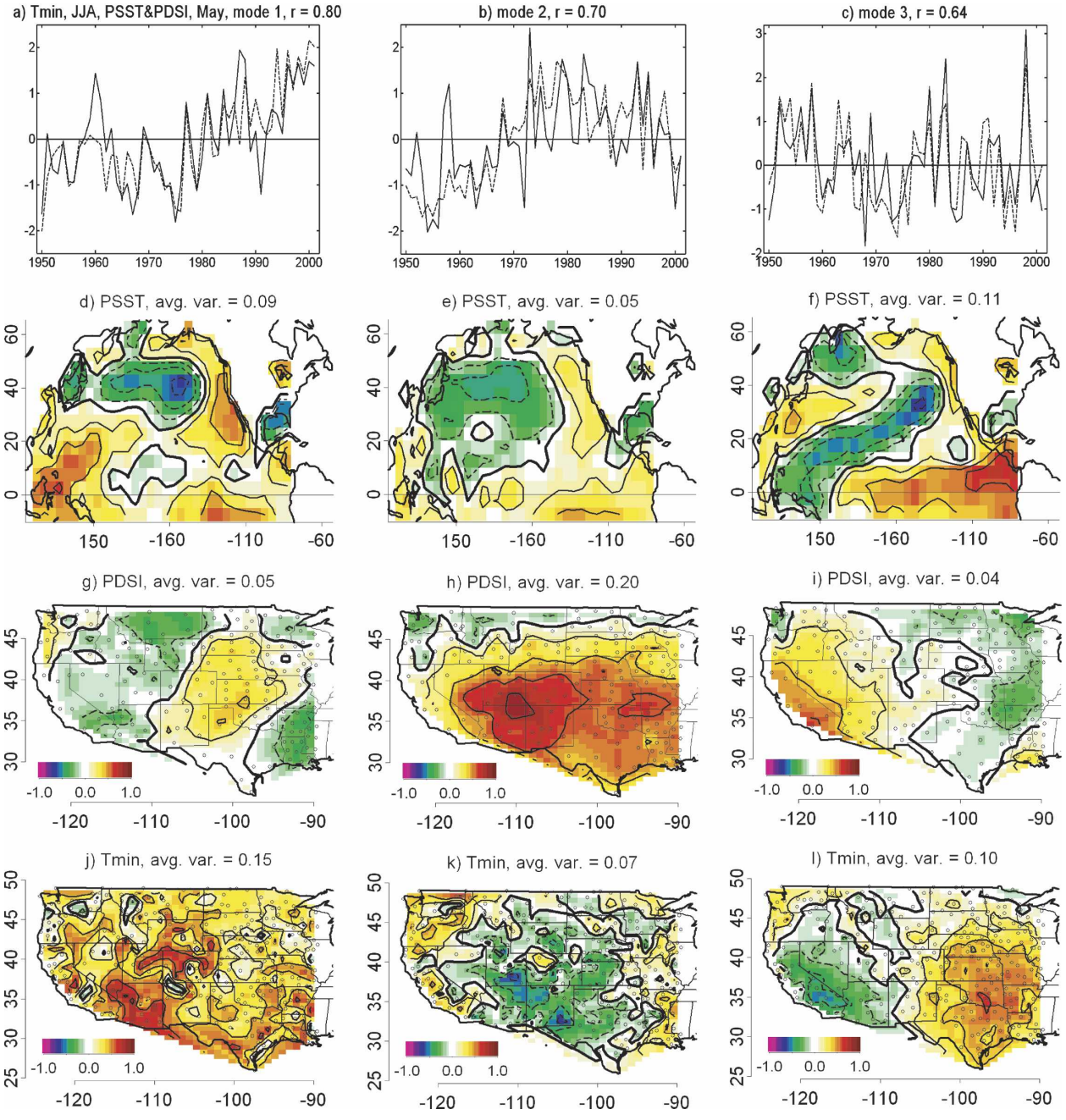

FIG. 8. Same as in Fig. 4, but for May PSST and PDSI. The correlations between the series are (a) 0.80, (b) 0.70, and (c) 0.64.

same predictors in May (Fig. 6b; maps not shown). Contrasting Figs. 10a and 9a, we notice that Tmin prediction has a rather robust pattern of positive and significant skill over a broader area than Tmax. These results agree and support the ones shown in Fig. 6 for JJA Tmin average skill, in which the inclusion of PSST predictors extended the memory of Tmin predictions (Fig. 6b). Mo (2003), found that mean temperature average skill tends to increase with SST lead time. We found this for Tmin but not in a consistent way for Tmax, as will be commented on later in this section.

Our average skill values for all PSST and PDSI predictor lags in the JJA Tmin prediction (~0.30, Fig. 6b) are comparable with those obtained for average temperature by Mo (2003) using a somewhat different linear ensemble canonical correlation methodology that included global SST, Northern Hemisphere sea level pressure, and seasonal model-estimated soil moisture

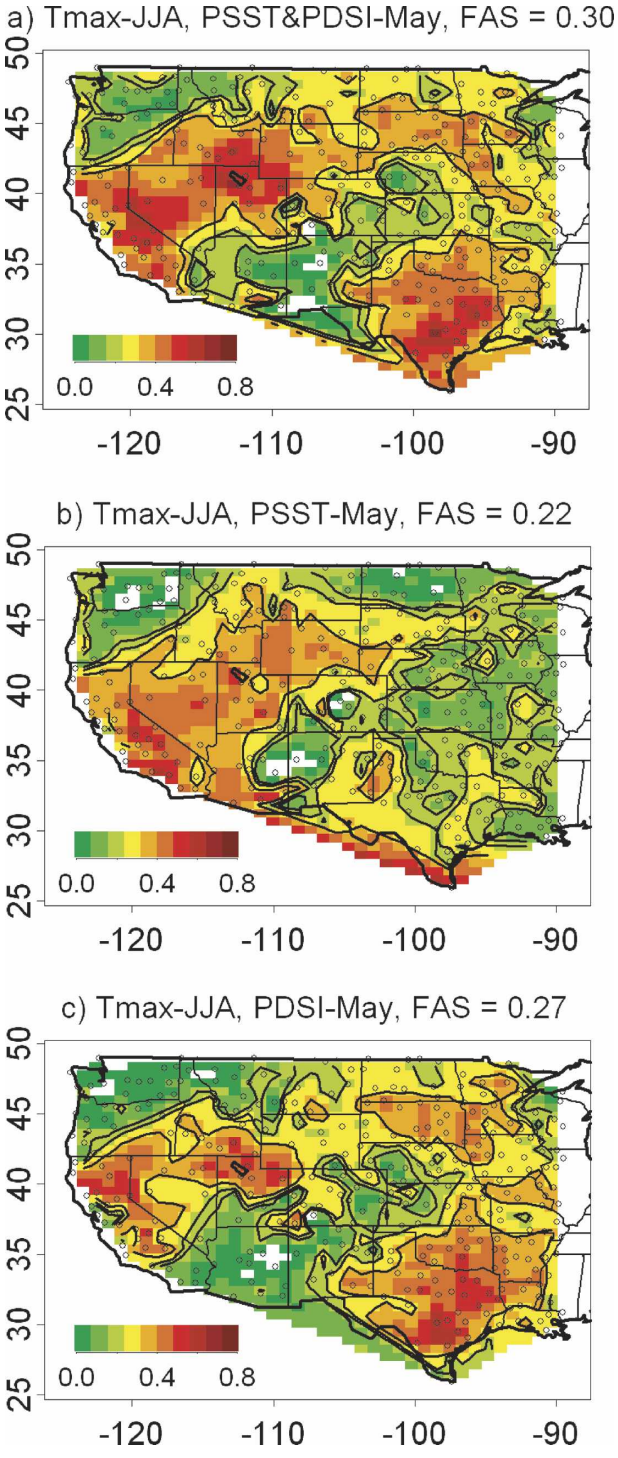

FIG. 9. JJA Tmax prediction skill expressed as correlations between the cross-validated forecast and observation time series. Uncolored areas are regions of insignificant negative correlations. Skill maps are using May (a) PSST and PDSI, (b) PSST, and (c) PDSI as predictors. The three contours plotted surround and represent the 90th, 95th, and 99th percent levels of significance in order of increasing correlations.

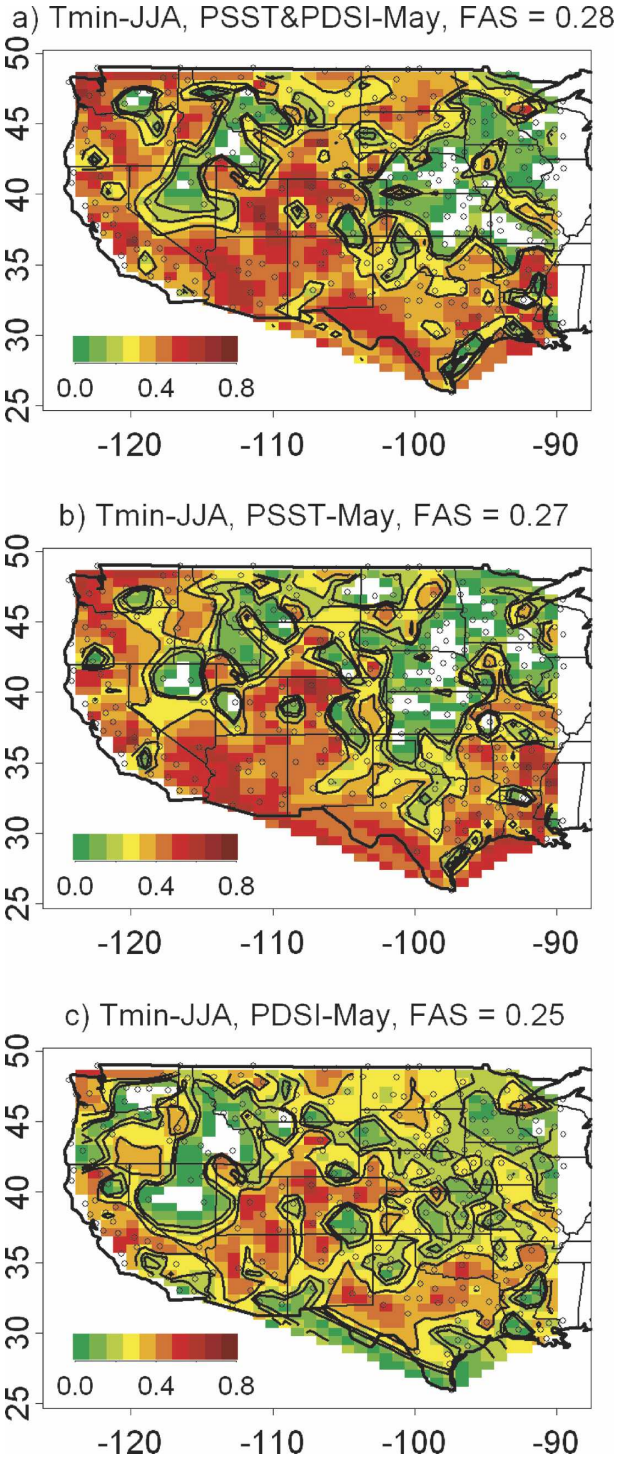

FIG. 10. Same as in Fig. 9, but for Tmin.

over the conterminous United States. In our results for JJA Tmax predicted from May PSST and PDSI, skill levels are similar to those found for Tmean by Mo (2003), but evidently the soil moisture influence upon

Tmax erodes more quickly with lead time than for Tmean or Tmin, as skill levels decay significantly for time lags of 3 and 5 months.

In comparing summer temperature specification and prediction with the other seasons, some interesting features emerged (Fig. 6). At time lags up to 3 months, soil moisture appears to influence Tmax and to some extent Tmin during a broad "season" from April through October. Interestingly, the highest predictive skills that emerged for these shorter time lags were for the spring (MAM) portion of this record. This seems to agree with findings of Van den Dool et al. (2003), who also found that MAM is the best predicted U.S. Climate Divisions mean temperature season.

Contemporaneous associations were especially strong for Tmax, with explanatory power almost entirely provided by PDSI; evidently this reflects rather strong coupling between the land surface and the surface air temperature, consistent with previous studies of mean temperature predictability by Huang et al. (1996) and Mo (2003). At time leads beyond 3 months, the influence of anomalous land surface characteristics falls away, but the more distant teleconnective influences of PSST persist at levels that are nearly the same as for 1-month predictions. An indication of the seasonal nature of the land surface influence is the fact that during cold seasons, most skill is obtained from the PSST predictors. This is coherent with Mo (2003), who found that the main sources for temperature prediction during winter are decadal PSST signals and ENSO. When both PDSI and PSST predictor fields are included, spring and summer Tmin can be better predicted than Tmax for long lead times.

c. *Results for summer frequency of daily Tmax extremes*

A summary of predictability and specification results for the frequency of very hot summer days (JJA Tmax90) is shown in Fig. 11. These results support and echo those for JJA Tmax in that the highest skill values are achieved using either PDSI or PSST and PDSI predictors at short lead times and also that the importance of PSST predictors increases with lead time. The latter result is also similar to that found for Tmin. For all lead times and predictors, somewhat better skill results were obtained for Tmax when compared with Tmax90. This is natural: extremes are typically more difficult to predict than the means. However, at 1-month lead time with PDSI as sole predictor, predictability of Tmax90 is almost identical to that of Tmax in both spatial pattern and skill magnitude (Fig. 9c). This result is encouraging, as many practical applications require skillful seasonal forecasts of extremes, not only the means. Among such variables, frequencies of hot days in summer are especially important for energy, health, and ecological applications.

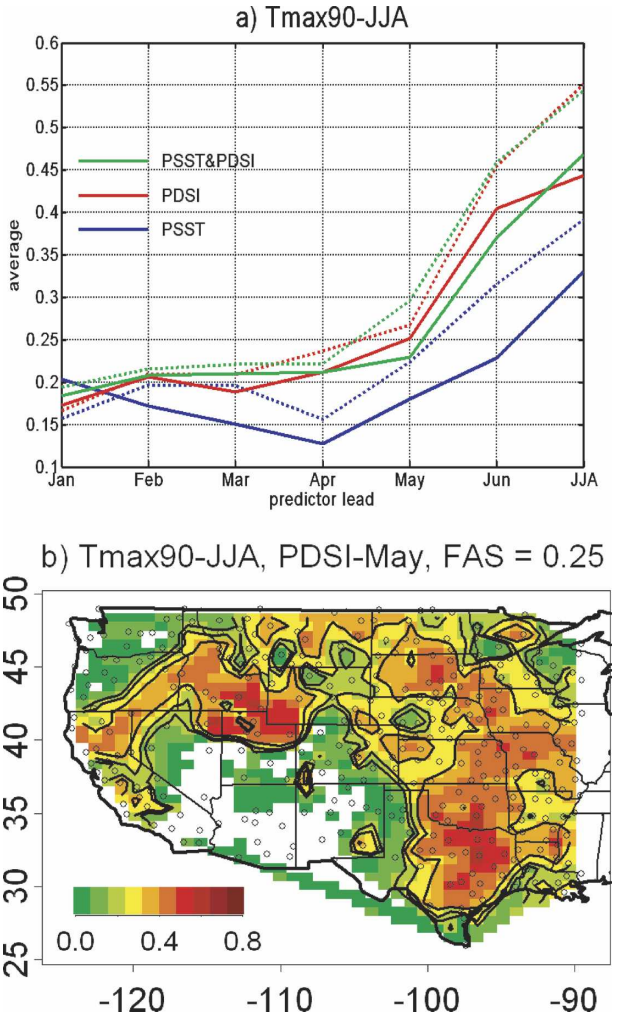

FIG. 11. (a) Tmax90 FAS for JJA, with June as the first month of the contemporaneous season and the five previous lagged months (e.g., from January to May) before JJA. Solid lines show skill levels for different sets of predictors used: PSST (blue), PDSI (red), and PSST and PDSI (green). For comparison, JJA Tmax skill is shown by dashed lines, with same colors for the different sets of predictor fields. (b) Tmax90 prediction skill expressed as correlations between the cross-validated forecast and observations at stations for JJA using May PDSI as predictor field. Uncolored areas are regions of insignificant negative correlations. The three contours plotted surround and represent the 90th, 95th, and 99th percent levels of significance in order of increasing correlations.

7. Summary and conclusions

Even though anomalous climate patterns are stronger and broader in scale in winter than in summer, summer surface air temperatures over the central and western portion of the United States appear to be more

predictable than those in winter. One reason for this important distinction is that, in addition to large-scale climate patterns, local soil moisture conditions provide a source of temperature (especially daytime temperature) predictability in summer. Therefore, two distinctly different variables, the Palmer Drought Severity Index (PDSI) and Pacific sea surface temperature (PSST), were explored using cross-validated, optimal-mode canonical correlation models for seasonal climate prediction. We found that PDSI and PSST provide useful skill in explaining and predicting the variability of summer temperatures at seasonal time leads. Importantly, PDSI and PSST have somewhat different influences upon Tmax and Tmin. Quite strong negative correlations occur between anomalous PDSI and Tmax locally, an indication that increased soil moisture and probably also cloudiness produce lower daytime temperatures. PDSI and Tmin are negatively correlated, but at considerably lower levels. Large-scale and remote climate conditions exert their influence on summer temperature variability and predictability in the central and western United States mainly through nighttime temperature.

Our linear statistical results indicate that, at a few months time leads, summer Tmax and Tmax90 predictability is controlled mainly by local effects, while the predictability of Tmin is related to both local and large-scale effects. For Tmax, soil moisture has the greatest influence especially in the Great Plains and other interior regions. For Tmin, PDSI contributes to predictive skill, but remote influences of PSST also come into play. The PDSI influence on Tmax is relatively strong in spring, summer, and early fall, but not in winter. PSST tends to have relatively greater influence (than PDSI) as time leads are increased and during cool season months. Douville (2003) and Van den Dool et al. (2003) suggest that although soil moisture is the main land surface parameter affecting the interannual variability of the summer atmosphere, a proper evaluation of its predictability role can only be made when the variability of the SST is also considered.

As in Mo (2003), our study suggests that SST and PDSI both account for mean temperature predictability but we show that they have different influences upon daytime (Tmax) and nighttime (Tmin) temperatures, and they have different regional expressions. Usually the best field average skill is obtained when using both predictors. At monthly time lead, summer Tmax predictive skill is strongest in regional clusters in the previously recognized Southern Plains area of Texas, Oklahoma, and Missouri, but also in California and from Nevada northeastward to South Dakota. Although the strongest soil moisture influence on daily maximum temperatures occurs in the interior portion of the western domain, this local influence occurs throughout most of the West. In contrast to that for Tmax, predictive skill for Tmin is more spatially widespread, with comparable influence exerted by PDSI and PSST.

Including PDSI to SST-based predictive models is more important for warm (April through October) than for cool (November through March) seasons, but the skillfully predictable regions found for Tmax are not necessarily coincident with those for Tmin. This investigation of the variability of Tmax and Tmin separately sheds light on the sources of predictability for average temperature examined by Mo (2003). For example, Tmin predictability over the southwestern monsoon region is associated mainly with PSST variability, while most of the Tmax predictability that is centered over the Plains region is associated with PDSI variability. In contrast to the PSST connection to Tmin, which appears to operate through the involvement of remote atmospheric teleconnections, the PDSI influence upon Tmax seems to operate locally or regionally via land surface processes.

Importantly, high-frequency extreme temperature, in this case the seasonal frequency of daily Tmax above the 90th percentile of the climatological JJA Tmax distribution (Tmax90), also exhibits predictive skill. This skill is comparable in spatial pattern and magnitude to that of average summertime Tmax skill achieved at monthly lead times. Like seasonal average Tmax, summertime frequency of extremely hot days (Tmax90) is mainly controlled by local soil moisture (PDSI) influences. At increasing lead times, remote large-scale climatic conditions play an ever-increasing predictive role. In any case, the demonstrated predictability of Tmax90, an important variable for numerous applications, gives us increased confidence in the practical usefulness of the seasonal predictability results described here.

Applications of the results for Tmax90 and Tmax are particularly important, because summer peak energy occurs in response to heavy loads from air conditioners, pumping water and other daytime temperature issues. Applications of the results for Tmin may be relevant to ecosystem and agricultural concerns. Cooler-than-average temperatures in spring or early summer could affect the planting or production of several crops, for example, wheat, sorghum, oats, and barley. These results indicate that more information is obtained for applications to the utility sector when Tmax and Tmin are considered separately rather than lumped into a mean temperature forecast. The results provide optimism that there may be predictability in other middle-lati-

tude regions, because the land surface influence is local, and thus there should be some skill derived from soil moisture memory. Unfortunately, few world regions outside of the Pacific sector could benefit from climatic predictability due to large-scale teleconnections because most climate modes are not as predictable or persistent as ENSO and PDO.

Acknowledgments. This work was conducted during the first author's visit to the Climate Research Division, Scripps Institution of Oceanography, University of California, San Diego. Funding was provided by the California Climate Change Center, sponsored by the California Energy Commission's Public Interest Energy Research Program, by the NOAA Office of Oceanic and Atmospheric Research under the California Energy Security Project, Grant NA17RJ1231, and by the NOAA Office of Global Programs, under the California Applications Program.

REFERENCES

Alley, W., 1984: The Palmer Drought Severity Index: Limitations and assumptions. *J. Climate Appl. Meteor.,* **23,** 1100–1109.

Barnett, T., 1981: Statistical prediction of North American air temperatures from Pacific predictors. *Mon. Wea. Rev.,* **109,** 1021–1041.

——, and R. Preisendorfer, 1987: Origins and levels of monthly and seasonal forecast skill for United States surface air temperatures determined by canonical correlation analysis. *Mon. Wea. Rev.,* **115,** 1825–1850.

Barnston, A., and T. Smith, 1996: Specification and prediction of global surface temperature and precipitation from global SST using CCA. *J. Climate,* **9,** 2660–2697.

Dai, A., K. E. Trenberth, and T. Qian, 2004: A global dataset of Palmer Drought Severity Index for 1870–2002: Relationship with soil moisture and effects of surface warming. *J. Hydrometeor.,* **5,** 1117–1130.

Delworth, T., and S. Manabe, 1988: The influence of potential evaporation on the variability of simulated soil wetness and climate. *J. Climate,* **1,** 523–547.

——, and ——, 1989: The influence of soil wetness on near-surface atmospheric variability. *J. Climate,* **2,** 1447–1462.

Douville, H., 2003: Assessing the influence of soil moisture on seasonal climate variability with AGCMs. *J. Hydrometeor.,* **4,** 1044–1066.

Durre, I., J. Wallace, and D. Lettenmaier, 2000: Dependence of extreme daily maximum temperatures on antecedent soil moisture in the contiguous United States during summer. *J. Climate,* **13,** 2641–2651.

Ebisuzaki, W., 1997: A method to estimate the statistical significance of a correlation when the data are serially correlated. *J. Climate,* **10,** 2147–2153.

Gershunov, A., and D. Cayan, 2003: Heavy daily precipitation frequency over the contiguous United States: Sources of climate variability and seasonal predictability. *J. Climate,* **16,** 2752–2765.

Groisman, P., R. Knight, T. Karl, D. Easterling, B. Sun, and J. Lawrimore, 2004: Contemporary changes of the hydrological cycle over the contiguous United States: Trends derived from in situ observations. *J. Hydrometeor.,* **5,** 64–85.

Heddinghaus, T. R., and P. Sabol, 1991: A review of the Palmer Drought Severity Index and where do we go from here? *Proc. Seventh Conf. on Applied Climatology,* Dallas, TX, Amer. Meteor. Soc., 242–246.

Heim, R. R., Jr., 2002: A review of twentieth-century drought indices used in the United States. *Bull. Amer. Meteor. Soc.,* **83,** 1149–1165.

Higgins, R., and Coauthors, 2003: Progress in Pan American CLIVAR Research: The North American Monsoon System. *Atmosfera,* **16,** 29–65.

Huang, J., and H. Van den Dool, 1993: Monthly precipitation–temperature relations and temperature prediction over the United States. *J. Climate,* **6,** 1111–1132.

——, ——, and K. Georgakakos, 1996: Analysis of model-calculated soil moisture over the United States (1931–1993) and applications to long-range temperature forecasts. *J. Climate,* **9,** 1350–1362.

Kaplan, A., M. A. Cane, Y. Kushnir, A. C. Clement, M. B. Blumenthal, and B. Rajagopalan, 1998: Analysis of global sea surface temperatures 1856–1991. *J. Geophys. Res.,* **103,** 18 567–18 589.

Koster, R., and M. Suarez, 2003: Impact of land surface initialization on seasonal precipitation and temperature prediction. *J. Hydrometeor.,* **4,** 408–423.

——, ——, and M. Heiser, 2000: Variance and predictability of precipitation at seasonal-to-interannual timescales. *J. Hydrometeor.,* **1,** 26–46.

Lawrimore, J., R. Heim Jr., M. Svodoba, V. Swail, and P. Englehart, 2002: Beginning a new era of drought monitoring across North America. *Bull. Amer. Meteor. Soc.,* **83,** 1191–1192.

Mantua, N., S. Hare, Y. Zhang, J. Wallace, and R. Francis, 1997: A Pacific interdecadal climate oscillation with impacts on salmon production. *Bull. Amer. Meteor. Soc.,* **78,** 1069–1079.

Mo, K., 2003: Ensemble canonical correlation prediction of surface temperature over United States. *J. Climate,* **16,** 1665–1683.

NCDC, 2003: Data documentation for data set 3200 (DSI-3200): Surface land daily cooperative summary of the day. National Climatic Data Center, Asheville, NC, 36 pp. [Available online at http://www.ncdc.noaa.gov/pub/data/documentlibrary/tddoc/td3200.pdf.]

Palmer, W., 1965: Meteorological drought. U.S. Department of Commerce Weather Bureau Research Paper 45, 58 pp.

Reynolds, R., and T. Smith, 1994: Improved global sea surface temperature analyses using optimum interpolation. *J. Climate,* **7,** 929–948.

Shabbar, A., and W. Skinner, 2004: Summer drought patterns in Canada and the relationship to global sea surface temperatures. *J. Climate,* **17,** 2866–2880.

Van den Dool, H., J. Huang, and Y. Fan, 2003: Performance and analysis of the constructed analogue method applied to U.S. soil moisture over 1981–2001. *J. Geophys. Res.,* **108,** 8617, doi:10.1029/2002JD003114.

Yang, F., A. Kumar, and K. M. Lau, 2004: Potential predictability of U.S. summer climate with "perfect" soil moisture. *J. Hydrometeor.,* **5,** 883–895.